A stable fluid rigid body interaction algorithm: application to industrial problems

D. Abouri, A. Parry, Aziz Hamdouni

A STABLE FLUID RIGID BODY INTERACTION ALGORITHM: APPLICATION TO INDUSTRIAL PROBLEMS

D. ABOURI
CD Adapco Group , 31 rue Delizy, 93698 Pantin Cedex, France
e-mail: driss_abouri@yahoo.fr

A. PARRY
Schlumberger - Riboud Product Center, 1 rue Henri Becquerel, 92140 Clamart, France
e-mail: aparry@clamart.oilfield.slb.com

A. HAMDOUNI
University of La Rochelle, LEPTAB, Av. Michel Crépeau, 17042 La Rochelle, France
e-mail: ahamdoun@univ-lr.fr

ABSTRACT

Fluid-mechanism interactions occur in a wide range of flow meter categories including turbine and positive displacement systems as well as many flow control devices. This paper outlines computational methods for calculating the dynamic interaction between moving parts and the flow in a flow meter system. Coupling of phenomena is allowed without need for access to the source codes and is thus suitable for use with commercially available codes. Two methods are presented one with an explicit integration of the equations of motion of the mechanism and the other with implicit integration. Both methods rely on a Navier-Stokes equation solver for the fluid flow. The more computationally expensive implicit method is recommended for mathematically stiff mechanisms such as piston movement. Example industrial applications shown are for positive displacement machines and axial turbines. The advances in mesh technology including deforming meshes with non-conformal sliding interfaces opens up this new field of application for Computational Fluid Dynamics and mechanical analysis in flow meter design.

INTRODUCTION

There are many different groups of flow metering devices [1], some of which include moving parts such as turbines and positive displacement meters and some which are static for example ultrasonic, fluidic and pressure drop based systems. In the present note we describe the application of CFD and mechanical analysis in the study of transient fluid-structure interaction in measuring elements or flow control devices comprising moving parts and in particular where the moving parts play an important role in the measurement or control. We restrict the explanation to the case where the components that move relative to each other do not undergo internal deformation, that is the components are considered as rigid-bodies. However there is no limitation on the displacement of each rigid body. The principles developed are general and could be extended to include small or large internal deformations of the moving components. Applications of the methods described are made for an oscillating piston meter, a meter belonging to the positive displacement group.

A non-linear analysis to predict turbine-forced response is presented by Sayma et al. [2] using a coupling method of the fluid and structural models, the structural response is described by a linear model. Blom [3] investigated time-lagged schemes where coupling is included by sequential solutions of fluid and structure models. In an implicit variant the sequential solutions are repeated with interface boundary conditions updated until convergence is achieved. An algorithm is introduced to calculate fluid-structure interaction in a time marching fashion where both fluid and structure have to be integrated in time simultaneously.

In this paper two methods of coupling algorithm are explained. The theory necessary for fluid/rigid-body interaction calculations is developed in section 1. The explicit method and more computationally intensive implicit method, requiring the repetition of each time step, are explained. In section 2, an industrial application of the implicit coupling algorithm is given for the oscillating piston meter and the explicit scheme is employed to study the dynamics of an accelerating spinner used for flow indication. The fluid flow analysis software utilised for the calculations included in this paper was Star-CD [4].

1 DESCRIPTION OF CALCULATION METHODS

1.1 Fluid rigid body interaction problem

As described in figure 1, suppose that a fluid-structure interaction problem has to be solved, where the fluid occupies the domain Ω_F, and the solid body described in Lagrangian coordinates occupies the domain Ω_S. They have the common moving boundary $\Gamma(t) = \overline{\Omega}_F(t) \cap \overline{\Omega}_S(t)$ where the interaction takes place. On the remaining part of the boundaries Γ_f, Γ_f^u and Γ_f^σ we shall assume that appropriate boundary conditions have been specified, which make the whole problem well-posed.

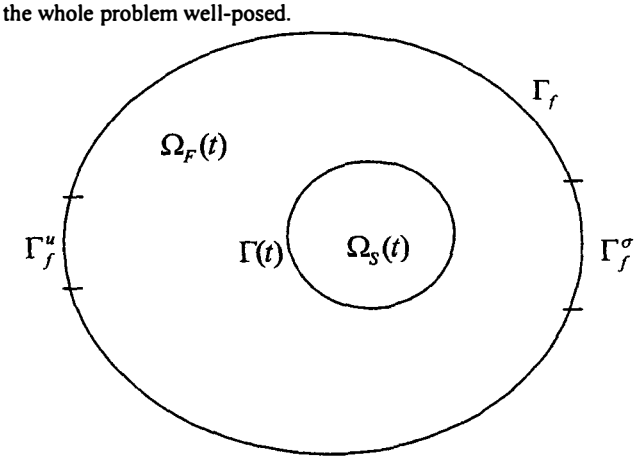

FIG. 1 : Diagram showing fluid and solid domains

If one assumes the fluid is incompressible, the flow field variables are calculated from a set of equations which express in the spatial fluid domain Ω_F the conservation of fluid momentum and volume, the Navier-Stokes equations as follows :

$$\begin{cases} div\, u = 0 \\ \rho_f \left(\dfrac{\partial u}{\partial t} + u \cdot \nabla u \right) = div\, \sigma_F + f \end{cases} \quad (1)$$

The body moves due to flow-induced forces, in addition to fluid flow, one has to compute the body motion by solving the equations of motion (in general six degrees of freedom) :

$$\begin{cases} m \dfrac{dv_G}{dt} = F_S + F_f \\ J \dfrac{d\omega}{dt} + \omega \times (J\omega) = M_S + M_f \end{cases} \quad (2)$$

where J is the operator of inertia of the solid S in the centre of inertia (written in a reference frame related to the solid), m is the mass of the solid, F_S is the resultant of the external efforts solid/solid and gravity.

The surface forces (pressure and shear) exerted by the fluid on the solid are given by :

$$\vec{F}_f = \int_\Gamma \sigma_F \cdot n_S d\gamma$$

where σ_F is the constraint of Cauchy in the fluid :

$$\sigma_F = -pI + \upsilon \left(\nabla u + {}^t \nabla u \right)$$

and the moment of the efforts exerted by the fluid on the solid, to the centre of inertia G, is given by :

$$\vec{M}_f = \int_\Gamma \overrightarrow{GM} \times \sigma_F \cdot n_S d\gamma$$

As the solid is rigid,

$$\forall M \in \Gamma(t),\ v(M) = v(G) + \omega \times \overrightarrow{GM}$$

The condition of non-slip is thus written as follow :

$$\forall x \in \Gamma(t)\ ,\ u(x) = v(G) + \omega \times x$$

In addition, we have to have force equilibrium across the interface :

$$\sigma_F \cdot n_{|\Gamma(t)} = \sigma_S \cdot n_{|\Gamma(t)}$$

where $n_{|\Gamma(t)} = n_{S|\Gamma(t)} = -n_{F|\Gamma(t)}$, is the unitary normal vector of the solid wall Γ.

1.2 Arbitrary Lagrangian Eulerian Formulation

In continuum mechanics one can describe fluid motion with two classical formulations. In the Lagrangian approach, the independent variables are taken to be the initial position, a, of a material point and time t. Lagrangian description prove extremely useful in large deformation problems in solid mechanics. Nevertheless, this formulation include severe distortions as the mesh deform with the material.

In the Eulerian description, the independent variables are spatial position x and time t. Eulerian approach are most often used in fluid mechanics. The mesh is fixed in space so the description undergo no distortion due to material motion.

For problems involving moving wall boundaries, it is necessary to have a middle formulation following the boundary motion and preserving the volume shape in the same time. To enable the computational mesh to remain regular even in presence of large structure displacements, Arbitrary Lagrangian-Eulerian formulation (ALE) has been introduced by by Noh [5] and Hirt et al. [6] for finite difference formulation. Hughes et al. [7], Belytschko et al. [8], Liu et al. [9], Benson [10] introduced the Finite element ALE formulation for incompressible viscous flows. Recently, the ALE method has been successfully applied to such moving boundary problems considering a rigid body structure [11] and [12]. The aim of the ALE formulation is to capture the advantages of both Lagrangian and Eulerian description while minimizing the disadvantages. The equations of motion are written in a form which accounts for the relative motion of the grid with respect to the fluid.

In the ALE description, each node is defined by the co-ordinates χ. The figure 2 define domains in space and associated mappings from one domain to another.

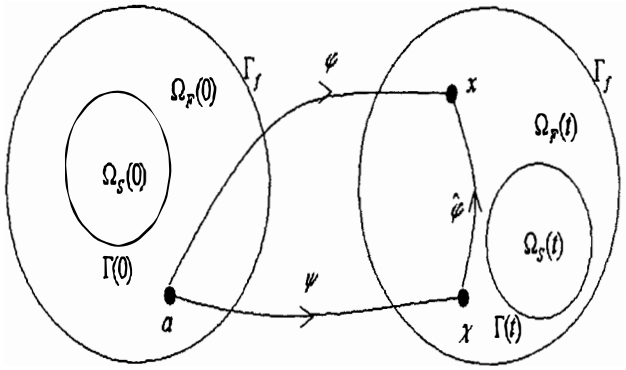

FIG. 2 : Representation of Eulerian, Lagrangian and Arbitrary reference domains

Therefore, the mapping φ relate the Eulerian and Lagrangian space reference co-ordinates :

$$x = \varphi(a,t)$$

Consider a physical property $g(x,t)$ expressed in the spatial representation :

$$g(x,t) = g(\varphi(a,t),t) = \tilde{g}(a,t) \quad (3)$$

Now taking the time derivative of (3) with the material co-ordinates held fixed, we get :

$$\dot{g} = \left.\frac{\partial \tilde{g}}{\partial t}\right|_a = \left.\frac{\partial g}{\partial t}\right|_x + u \cdot \nabla_x g \quad (4)$$

where $u = \left.\dfrac{\partial x}{\partial t}\right|_a$ is the material velocity.

Therefore, the mapping φ relate the Eulerian and ALE space reference co-ordinates :

$$x = \hat{\varphi}(\chi,t)$$

Thus the physical property $g(x,t)$ can be expressed in the spatial representation as follow :

$$g(x,t) = g(\hat{\varphi}(\chi,t),t) = \hat{g}(\chi,t) \quad (5)$$

with the following time derivative expression :

$$\dot{g} = \left.\frac{\partial \hat{g}}{\partial t}\right|_{\chi} = \left.\frac{\partial g}{\partial t}\right|_{x} + w \cdot \nabla_x g \tag{6}$$

where $w = \left.\frac{\partial x}{\partial t}\right|_{\chi}$ is the mesh velocity.

Finally, we obtain a fundamental relationship which enables us to translate any law expressed in material (Lagrangian) variables into an equivalent law expressed in mixed variables :

$$\dot{g} = \overset{\circ}{g} + (u - w) \cdot \nabla_x g \tag{7}$$

The arbitrary Lagrangian-Eulerian description may thus be viewed as a mapping of the initial configuration of the continuum into the current configuration of the reference frame. The Jacobian determinant $J = \det\left(\frac{\partial \varphi}{\partial a}\right)$ provides a link between mixed and material coordinates.

The Jacobian J relates the current volume element dV in the spatial frame to the associated volume element dV_0 in the referential frame :

$$dV = J(a,t)dV_0, \text{ where J(a,0)=1}$$

One may show that the time rate of change of the mixed Jacobian is given by

$$J = \det\left(\frac{\partial \varphi}{\partial a}\right)$$

Consider a material co-ordinate a taken to be the initial position, we get :

$$J(a,t)\rho_f(\varphi(a,t),t) = \rho_0(a)$$

that we write :

$$J\rho_f = \rho_0$$

using the time derivative, we get mass conservation law :

$$\dot{\rho}_f + \rho_f \, div\, u = 0 \tag{8}$$

Using this law and relation (7), we obtain the expression in the ALE formulation :

$$\overset{\circ}{\rho}_f + (u - w) \cdot \nabla_x \rho_f + \rho_f \, div\, u = 0 \tag{9}$$

Using the same approach, we obtain momentum conservation law expressed in the ALE formulation.

In Eulerian form, we get :

$$\rho_f \left(\left.\frac{\partial u}{\partial t}\right|_{x} + u.\nabla u\right) = div\, u + f$$

using the relation (7) for the physical property u, we obtain :

$$\dot{u} = \left.\frac{\partial u}{\partial t}\right|_{x} + u.\nabla u = \overset{\circ}{u} + (u - w) \cdot \nabla u$$

Finally equation (7) is a fundamental relationship which enables us to translate any law

expressed in spatial (Eulerian) variables into an equivalent law expressed in mixed (ALE) variables :

$$\rho_f \left(\overset{\circ}{u} + (u - w) \cdot \nabla u\right) = div\, u + f$$

Consider the relation :

$$u(x,t) = u(\hat{\varphi}(\chi,t),t) = u \circ \hat{\varphi}(\chi,t) \tag{10}$$

Now taking the time derivative of (10) with the mixed co-ordinates held fixed :

$$\dot{u} = \left.\frac{\partial u \circ \hat{\varphi}}{\partial t}\right|_{\chi}$$

If one assumes the fluid is incompressible, the mass and momentum conservation equations are formulated as follows :

$$\begin{cases} div_x\, u = 0 & \text{in } \Omega_F(t) \\ \rho_f \left(\left.\frac{\partial u}{\partial t}\right|_{\chi} + (u - w) \cdot \nabla_x\, u\right) = div_x\, \sigma_F + f & \text{in } \Omega_F(t) \end{cases} \tag{11}$$

The Geometric Conservation Law is invoked in the formulation in order to avoid errors induced by deformation of control volumes (see Thomas et al. [13] or Demirzic et al. [14]). The surface of a control volume V is described by S and the surface vector n. In the case of moving grids, the space-conservation law (SCL) has to be satisfied :

$$\frac{d}{dt}\int_V dV - \int_S w \cdot n dS = 0$$

To cope with large domain deformations and displacement, in addition to the ALE we need a means of treating sliding interfaces within the calculation domain of the fluid flow. Commercially available fluid flow solvers are available with both these essential features for calculating fluid dynamics phenomena in domains undergoing large displacement/deformation. These methods are usually based on finite element or finite volume formulations.

The option of arbitrarily moving the mesh in the ALE description offers interesting possibilities. In fact, moving boundaries can be tracked with the accuracy characteristic of Lagrangian methods and the interior mesh can be moved so as to avoid mesh distortion. Several procedures for updating the mesh are explained in the literature [15,16,17,18,19]. Here in our application, the mesh motion is prescribed a priori based on the known of the rigid-body boundaries calculated at every instant.

1.3 Fully implicit coupled iteration schemes

We assume that the domains for the the fluid have been discretised appropriately, and has to be solved in a time-implicit manner.

The rigid-body movement is described by a set of ordinary differential equations of the form :

$$\begin{cases} m\frac{dv}{dt} = F(v,x,t) \\ \frac{dx}{dt} = v \end{cases} \tag{12}$$

where v is the velocity and x is the position of the body.

In the context of transient fluid-rigid body interaction, we have the choice of either explicit or implicit time integration of these ordinary differential equations. An example of velocity equation explicit discretization is:

$$v_{n+1} = v_n + \Delta t \frac{F(v_n, x_n, t_n)}{m} \tag{13}$$

Certain problems are better solved using an implicit discretization, particularly for problems with sensitive force velocity behaviour, known as stiff problems in the mathematical sense. For stability reasons, we would also like a time-implicit procedure for the overall time step. An example of velocity equation implicit discretization is :

$$v_{n+1} = v_n + \frac{\Delta t}{2}\left(\frac{F(v_n, x_n, t_n) + F(v_{n+1}, x_{n+1}, t_{n+1})}{m}\right)$$

To calculate v_{n+1}, we have to solve a non linear system :

$$G(v_{n+1}) = v_{n+1} - v_n - \frac{\Delta t}{2}\left(\frac{F(v_n, x_n, t_n) + F(v_{n+1}, x_{n+1}, t_{n+1})}{m}\right) = 0$$

As is well known, in order to accelerate convergence the most widely used and most robust method for the solution of nonlinear system is Newton-Raphson method. It require the evaluation of derivatives that we approximate by finite differences. With the implicit method, we have to repeat the application of the above equations until convergence for each time step.

$$G(v_{n+1}) = 0$$

$$\begin{cases} v_{n+1}^0 \text{ initial guess} \\ v_{n+1}^{k+1} = v_{n+1}^k - \left[\nabla G(v_{n+1}^k)\right]^{-1} G(v_{n+1}^k) \end{cases} \quad (14)$$

The Newton's method is an iterative procedure. To begin the iterative procedure, usually the initial value v_{n+1}^0 is predicted by an explicit scheme of the same order or simply from the result of the last time step ($v_{n+1}^0 = v_n$). In our application, v_{n+1}^0 is predicted with an explicit Adams-Bashforth scheme of order two :

$$v_{n+1}^0 = v_n + \frac{\Delta t}{2}\left(3\cdot\frac{F(v_n, x_n, t_n)}{m} - \frac{F(v_{n-1}, x_{n-1}, t_{n-1})}{m}\right)$$

Below is the description of the fully implicit coupled iteration solution algorithm for nonlinear fluid-rigid body interaction problems :

1. Explicit prediction of the interface velocity $v_{n+1}^0 = (v_{|\Gamma})^{n+1}$:

$$v_{n+1}^0 = (v_{|\Gamma})^n + \frac{3}{2}\Delta t(a_{|\Gamma})^n - \frac{1}{2}\Delta t(a_{|\Gamma})^{n-1}$$

2. Prediction of the interface position $x_{n+1} = x_n + \Delta t\, v_{n+1}^k$

3. Fluid mesh motion displacement based on the interface position Γ_{n+1}

4. Computation of fluid flow problem at t_{n+1}

a. Kinematic compatibility condition on the interface : $(u_{|\Gamma})^{n+1} = (v_{|\Gamma})^{n+1}$

b. Computation of near-wall forces acting on the solid at t_{n+1}, $F_f^{n+1} = -\int_{\Gamma_{n+1}} \sigma_F^{n+1} \cdot n\, d\gamma$

5. Computation of solid problem at t_{n+1}

a. Forces equilibrium across the interface, $\sigma_F^{n+1} \cdot n_{|\Gamma_{n+1}} = \sigma_S^{n+1} \cdot n_{|\Gamma_{n+1}}$

b. Update the velocity v_{n+1}^k of the interface Γ_{n+1}

6. Check for convergence : If $\left\|v_{n+1}^k - v_{n+1}^{k-1}\right\| \le \varepsilon$, go to the next time step

Else we compute again 2,3,4,5 updating the new velocity v_{n+1}^k at t_{n+1} computed at step 5

To realise the repetitions of the same time step we used a restart technique for moving mesh problems automated with an operating system script. The calculation stages comprising initialisation, rigid body dynamic analysis, mesh movement and flow calculation are shown in the flow diagram in figure 3.

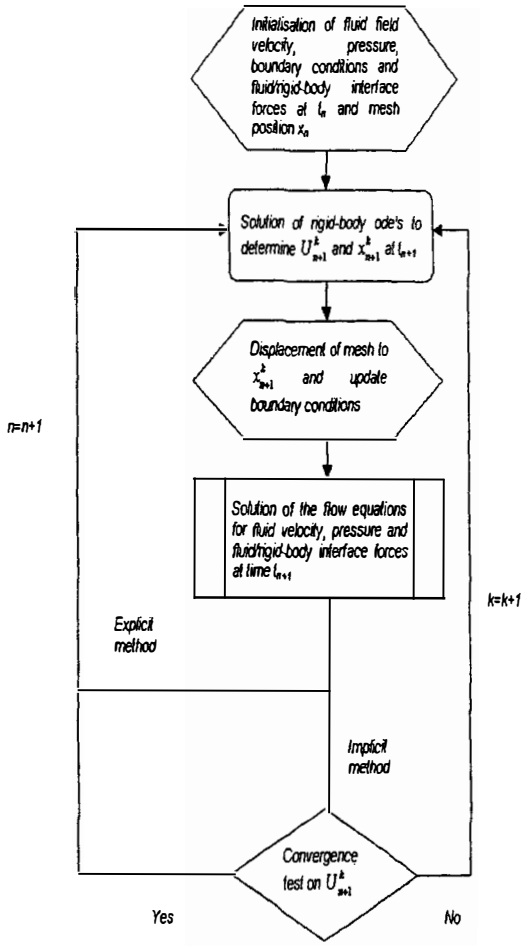

FIG. 3 : Flow diagram showing stages of fluid structure interaction calculation

1.4 Energy conserving and stability aspects

For fluid structure interaction problems with large displacements, it is necessary to have consistent and energy conservative interface boundary conditions at the moving fluid solid interface. The coupling algorithm have to be stable and the discretisation in time and space should respect the forces equilibrium at fluid solid interface. The fully implicit coupling algorithm developed in this paper respects this crucial property taking the real velocity field at interface as test function for convergence. When the structure is assumed to be rigid, Abouri [20] demonstrates that the fully implicit scheme verifes that the variation of the sum of the kinetic energy of the system is equal to the difference between the energy introduced by the external boundary conditions and the energy dissipated by viscous effects inside the fluid. Grandmont [21] demonstrates this principle of Energy conservation for the case of linear elastic structure.

Le Tallec et al. [22] proposes a stability demonstration for an implicit fixed point relaxation algorithm : it couples an implicit Euler treatment on the fluid domain and a mid-point rule for the structural equation. Similarly, Abouri [20] proposed a stability demonstration for the fully implicit coupling algorithm implemented here in the case of a rigid structure. The key point of the demonstration is to consider a global

continuum mechanics equation including both fluid and solid using variable functions for the physical quantities like density or velocity field.

If a simple explicit algorithm is used, we obtain a limitation in the time step and an instable response. The explicit method is first order accurate, but only conditionally stable. In fact, the explicit staggering algorithm does not conserve energy at the interface because at each timestep the energy introduced by the fluid loading σ_F^{n+1} on the structure is not equal to the energy change in the fluid. The difference between these two energies is $\int_{\Gamma^{n+1}} \sigma_F^{n+1}.(v_{n+1} - u_{n+1}) \cdot n d\gamma$.

For the explicit method, we have $(u_{|\Gamma})^{n+1} = (v_{|\Gamma})^n$. So the difference between the energies is $\int_{\Gamma^{n+1}} \sigma_F^{n+1}.(v_{n+1} - v_n) \cdot n d\gamma$ which is not equal to zero. The explicit coupling algorithm is not adequate to solve this type of problem because the delay between the two solvers fluid and structure creates energy dissipation. The kinematic condition implies equality of the velocities on the interface ($(u_{|\Gamma})^{n+1} = (v_{|\Gamma})^{n+1}$), the dynamic condition requires forces equilibrium across the interface ($\sigma_F^{n+1} \cdot n_{|\Gamma_{n+1}} = \sigma_S^{n+1} \cdot n_{|\Gamma_{n+1}}$). Those coupling conditions at the end of each new step are well fulfilled for the implicit scheme because of exchanging the coupling variables and updating of the fluid domain at each sub-iteration of each timestep. The implicit method can be very useful to solve the fluid and the structure at the same time and avoid energy dissipation creating by the delay between the two solvers created by an explicit method.

2 APPLICATION TO COMPLEX INDUSTRIAL FLOWS

2.1 Description of the Oscillating Piston Flow Meter [23]

The moving element consists of a hollow cylindrical piston with a horizontal web, contained within a cylindrical working-chamber provided with a cover as we see in figure 4.

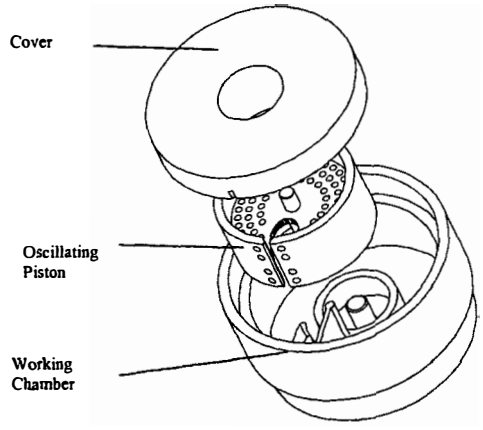

FIG. 4 : 3D view of Working Chamber and Oscillating Piston

A top view of an oscillating piston flow meter composed of a slotted piston which oscillates in a working chamber comprising a partition / guide plate is shown figure 5. A partition plate between inlet and outlet ports forces incoming liquid to flow around a cylindrical measuring chamber and through the outlet port. The motion of the oscillating piston in the unit is transferred to a magnetic assembly in the measuring chamber, which is coupled to a follower magnet on the other side of the chamber wall. In one cycle the angle θ undergoes one revolution. In fact it will be seen that the piston is always moving in the same direction and each revolution permits a certain volume of fluid to pass through the meter.

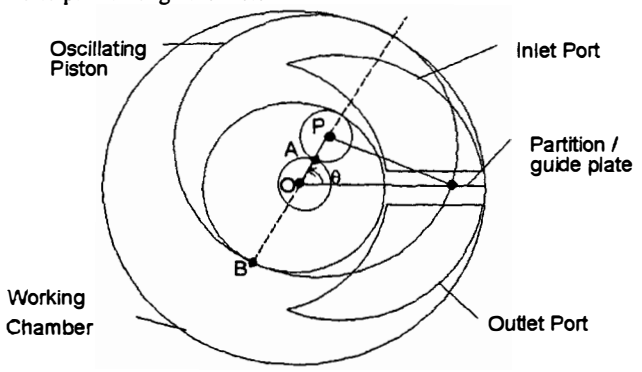

FIG. 5 : Schematic of an oscillating piston meter

2.2 Equations of motion of the mechanism, treatment of friction

The problem can be schematised by a slider-crank mechanism represented in figure 9. The connecting rod PQ is part of the oscillating piston.

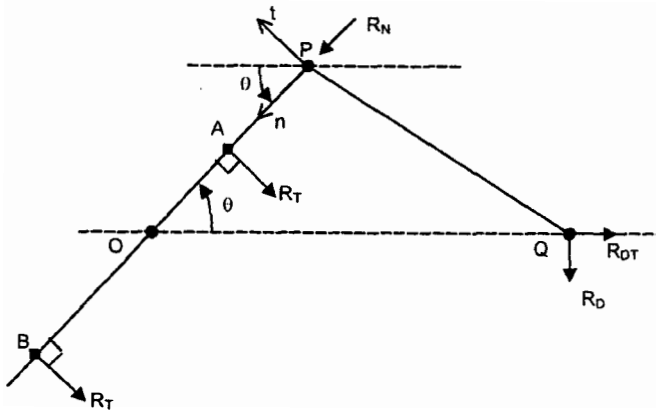

FIG. 9 : Free-body diagram of oscillating piston

Where

G = resultant body force due to weight according to the principle of Archimedes,
F = resultant hydrodynamic force,
M_F = resultant hydrodynamic moment about point O,
R = reaction forces acting on piston at contact lines,
M_C = reaction force moment about point O,
r_{OP} = distance between O and P,
m, I = mass, moment of inertia about P of piston.
The equations of motion in normal (n), tangential (t) and axial (z) coordinates about O are:

$$F'' + G'' + R'' = mr_{OP}\dot{\theta}^2$$
$$F' + G' + R' = mr_{OP}\ddot{\theta}$$
$$M_F^z + M_C^z = -\bar{I}^z\ddot{\beta} + mr_{OP}^2\ddot{\theta}$$

The friction in the n, t plane on the piston bottom or top surface can be expressed using the hypothesis that the repartition of the normal reaction force in the z direction is uniform. The choice of this treatment of friction for the plane contact on the bottom or top of the piston has proved to be useful when compared with experimental data.

2.3 Results of calculations

Inlet and outlet ports are positioned on the ends (top and/or bottom) of the working chamber to allow the 'positive displacement' of fluid. The guide plate serves also to isolate incoming and outgoing fluid.
Figure 10 shows the mesh interface between two domains of fluid, one static (the inlet and outlet parts) and one deforming (the annular chamber with piston).

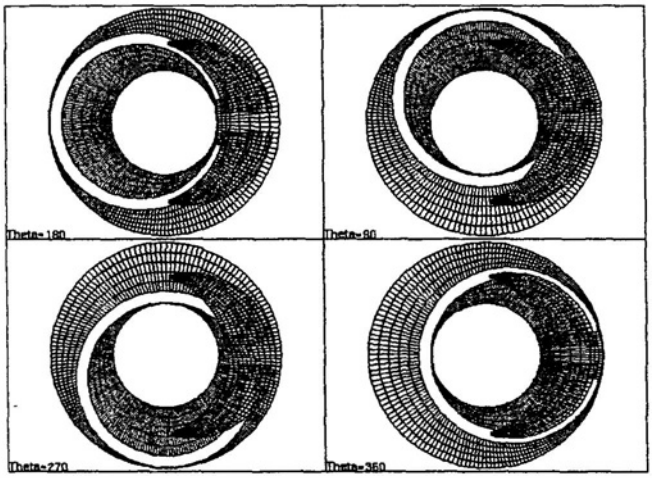

FIG. 10 : Evolution of mesh interface

Below are images of calculated results in an oscillating piston flow meter.
Figure 11 shows at left the velocity vectors in a plane through the meter and at right the contour pressure in a plane through the meter. We note the higher pressure (dark colour) in the inlet volumes to overcome piston friction, inlet/outlet losses and inertial effects.

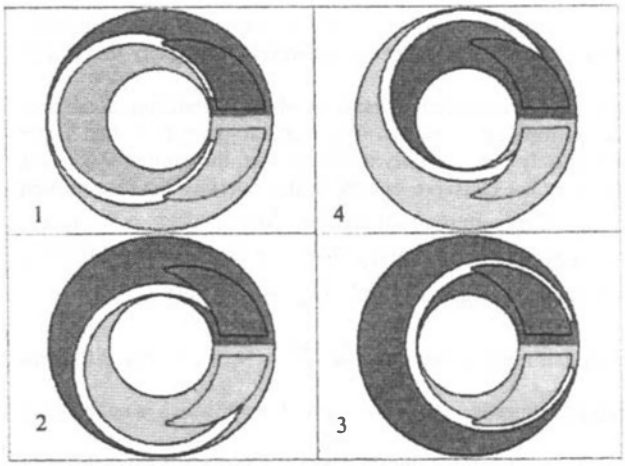

FIG. 11 : Piston movement cycle 1-2-3-4 : Dark regions representing high pressure inflow

The information available for the positive displacement meter using the implicit approach are simulated calibration curves, pressure drops, forces acting on the components and behaviour of meter in a time varying consumption profile. The experiments offer quantitative data for detailed validation of the numerical solution.
Figure 12 shows the calculated calibration curve compared with experimental data in water at standard conditions. Comparisons were within 1 percent which indicates the validity of the fully coupled implicit algorithm.

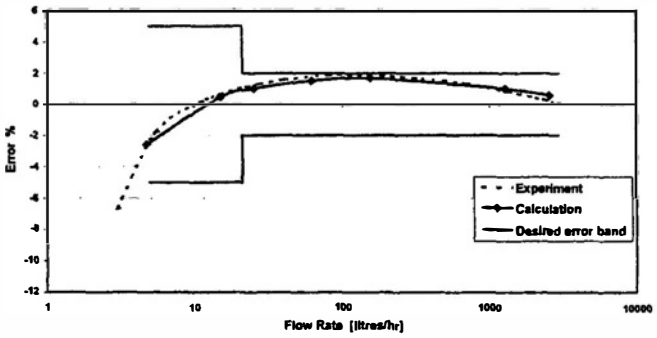

FIG. 12 : Comparisons of predicted frequency against the measured frequency

2.4 Time and space discretisation tests

To demonstrate the robustness of the solution algorithm, time step and grid size dependence tests were carried out with the same boundary conditions and at high flow rate.
We compare the rotating velocity of the piston induced by fluid forces.
We note N_r x N_θ x N_z CV the control volume number used with respectively N_r, N_θ and N_z subdivisions in the direction r, θ and z in the cylindrical reference frame related to the center of the box.
Calculations were performed on four numerical grids, one coarse with a 13 x 90 x 8 CV and one refined with a 26 x 270 x 16 CV.
For the coarsed one, three time increments were used : $\Delta t = T/82$,

$\Delta t = T/164$ and $\Delta t = T/328$. Here T represent the time period corresponding to one cycle of piston revolution.
Figure 13 shows a comparison of the rotating piston velocity calculated on the coarsed grid with three different time steps during a revolution of about T =0.0492 s. One does not observe a significant difference between the results, which indicates that the temporal errors are small.

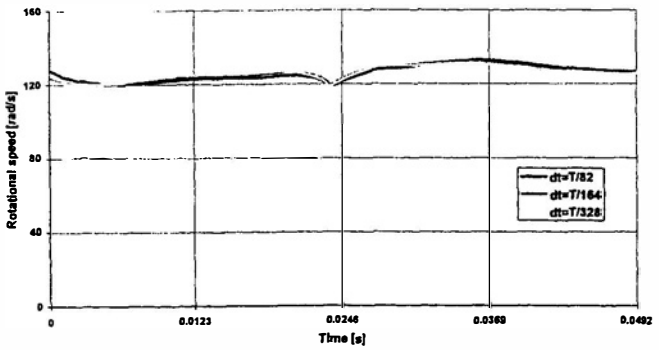

FIG. 13 : Comparison of predicted rotating piston velocity versus time using the coarse grid (13 x 90 x 8 CV) and various time steps

Figure 14 shows comparison between fine and coarse grid results during a revolution both obtained with $\Delta t = T/82$. As the grid is refined the results tend to the same solution. No significant differences exist, these comparisons show that the spatial discretization errors are small enough to demonstrate the robustness of the scheme.
Although for numerically accurate results for particle tracking for example, further grid refinement is necessary. But for predict pressure drop or calibration curves in the optic of an optimisation form of the product, the numerical accuracy achieved on the 13 x 180 x 8 CV and $\Delta t = T/82$ suffices.

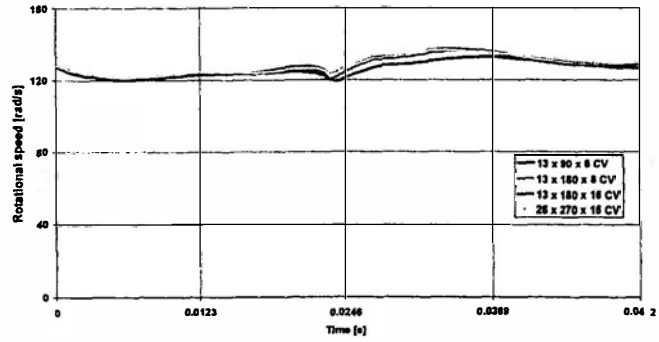

FIG. 14 : Comparison of predicted rotating piston velocity versus time using time step $\Delta t = T/82$ and various grids

2.5 Dynamics of a spinner in a conduit with water flow

The algorithm is used to calculate dynamic response of an axial flow spinner placed in a conduit used to indicate flow velocity. A lumped parameter analysis of such a spinner gives the classical equation:

$$I_{eff}\ddot{\theta} = \rho u A\left(\frac{\bar{r}u}{\tan\beta} - \bar{r}^2\dot{\theta}\right)$$

where I_{eff} is the effective moment of inertia including the mass of the fluid in the cylindrical volume swept by the blades, β is the blade outlet flow angle, $\dot{\theta}$ is the spinner angular velocity, u is the flow velocity, $\bar{r}$ is the effective blade radius, A is the area of a plane disc normal to the flow and bounded by the blade root and tip radii and ρ the density of the fluid. The solution of the above equation compares well with the results from the algorithm with explicit scheme. As shown in figure 15, the error at terminal conditions is about 5%.

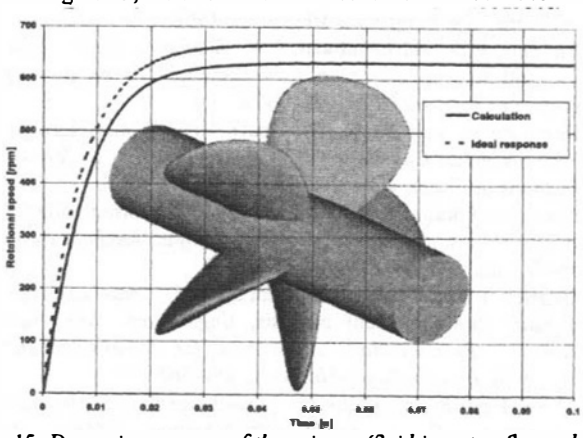

FIG. 15: Dynamic response of the spinner (fluid is water, flow velocity =1 m/s, initial spinner velocity=0 rpm, β=60 degrees, r=8 mm)

3 REFERENCES

1 BS-7405 Selection and application of flowmeters for the measurement of fluid flow in closed conduits. *British Standards Institution*, 1991

2 **Sayma, A. I., Vahdati, M.** and **Imregun, M.** Turbine forced response prediction using an integrated non-linear analysis. *Institution of Mechanical Engineers, Multi-body Dynamics Part K Vol 214 No K1*, 2000

3 **Blom, F.** A monolithical fluid-structure interaction algorithm applied to the piston problem. *J. Comput. Methods Appl. Mech. Engrg. 167*, 1998

4 **STAR-CD.** Methodology & User Guide. *Computational Dynamics Limited*, 1999

5 **Noh, W.F.** A time dependent two space dimensional coupled Eulerian Lagrangian code, *Meth. Comput. Phys. 3, Alder E. Fenbach and Rosenberg Editions*, 1964

6 **Hirt, C.W., Amsdern, A.A.** and **Cook, H.K.** An arbitrary Eulerian Lagrangian method for all flow speeds, *J. Comput. Phys., 14, 229-253*, 1974

7 **Hughes, T.J.R., Liu, W.K.,** and **Zimmermann, T.K.** Lagrangian-Eulerian finite element formulation for incompressible viscous flows, *Computer Methods in Applied Mechanics and Engineering, 29, 329-349*, 1981

8 **Belyschko, T., Flanagran, D.F.** and **Kennedy, J.M.** Finite element method with user-controlled meshes for fluid-structure interactions, *Comput. Methods Appl. Mech. Engrg., 33, 689-723*, 1982

9 **Liu, W.K.** and **Huerta, A.** Viscous flows for large free surface motion, *Comput. Methods Appl. Mech. Engrg., 69, 277-324*, 1988

10 **Benson, D.** An efficient accurate, simple ALE method for non linear finite element programs, *Comp Meth in Appl Mech and Eng, 33 689-723*, 1989

11 **Nomura, T.** and **Hughes, T.J.R.** An Arbitrary Lagrangian Eulerian finite element method for interaction of fluid and rigid body. *Comput. Methods Appl. Mech. Engrg.* **95**, 115-138, 1992

12 **Sarrate, J., Huerta, A.** and **Donea, J.** Arbitrary Lagrangian-Eulerian formulation for fluid-multi rigid bodies interaction problems. *Computational Mechanics,* 1998

13 **Thomas, P.D.** and **Lombard, C.K.** Geometric conservation law and its application to flow computations on moving grids, *AIAA Journal 17, 1030*, 1979

14 **Demirzic, I.** and **Peric, M.** Space Conservation Law In Finite Volume Calculations Of Fluid Flow. *Int. J. Numer. Methods in Fluids, 8, pp.1037-1050*, 1988

15 **Souli, M., Ouahsine, A.** and **Lewin, L.** ALE formulation for fluid-structure interaction problems, *Comput. Methods Appl. Mech. Eng. 190, pp. 659-675*, 2000

16 **Hughes, T.J.R.** The finite element method. Linear static and dynamic finite element analysis, *Englewood Cliffs, New Jersey : Prentice-Hall, Algorithms for hyperbolic and parabolic-hyperbolic problems, pp. 490-567*, 1987

17 **Blom, F.J.** Investigations on computational fluid-structure interaction, *Thèse, Ecole polytechnique fédérale de Lausanne*, 1998

18 **Van Leer, B.** Flux-Vector Splitting for the Euler Equations, *Proc. 8th Int. Conf. On Numerical Methods in Fluid Dynamics, Springer Verlag, pp. 507-512*, 1982

19 **Batina, J.T.** Implicit flux-split Euler schemes for unsteady aerodynamic analysis involving unstructured dynamic meshes, *AIAA J., 29, pp. 1836-1843*,1991

20 **Abouri, D.** A Fluid Rigid Body Interaction Algorithm : Application to Volumetric Flow Meter, *Thesis, University of Poitiers, France*, 2003

21 **Grandmont, C.** Analyse mathématique et numérique de quelques problèmes d'interaction fluide-structure, *Thèse, Université de Paris VI*, 1998

22 **Le Tallec, P.** and **Mouro, J.** Fluid structure interaction with large structural displacements, *Comp. Meth. in applied mechanics and engineering.*, **vol. 190,** no 24-25 , pp. 3039 – 3067, 2001

23 **Linford, A.** Flow Measurement & Meters. *N.Tetlow, London,* 1949